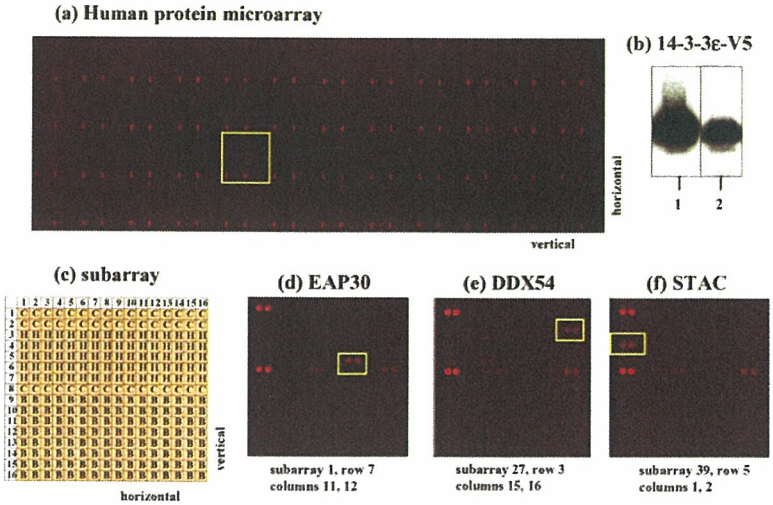

Fig. 1. Protein microarray analysis. (a) Human protein microarray. The microarray contains 1752 distinct human proteins of various functional classes spotted in duplicate on a nitrocellulose-coated glass slide. They are printed in an arrangement of 4 × 12 subarrays equally spaced in vertical and horizontal directions. A representative subarray is indicated by an enclosed yellow line. (b) Recombinant human 14-3-3ε protein tagged with V5. One microgram of the protein was processed for Western blot analysis using anti-V5 antibody (lane 1) or anti-14-3-3ε antibody (lane 2). (c) Layout of the subarray. Each subarray includes 16 × 16 spots composed of 48 control spots (C), 80 human proteins (H), and 128 blanks (B). The positive control spots include an Alexa Fluor 647-labeled antibody (rows 1, 8; columns 1, 2; strong signals), a concentration gradient of a biotinylated anti-mouse antibody with a capacity to bind to mouse monoclonal anti-V5 antibody conjugated with Alexa Fluor 647 (row 8; columns 3–8; signals visible on the higher concentration), and a concentration gradient of V5 protein (row 8; columns 13–16; signals visible on the higher concentration). (d) EAP30. (e) DDX54. (f) STAC. The three proteins indicated by an enclosed yellow line located on different subarrays (d–f) represent an example identified as showing significant binding to the probe.

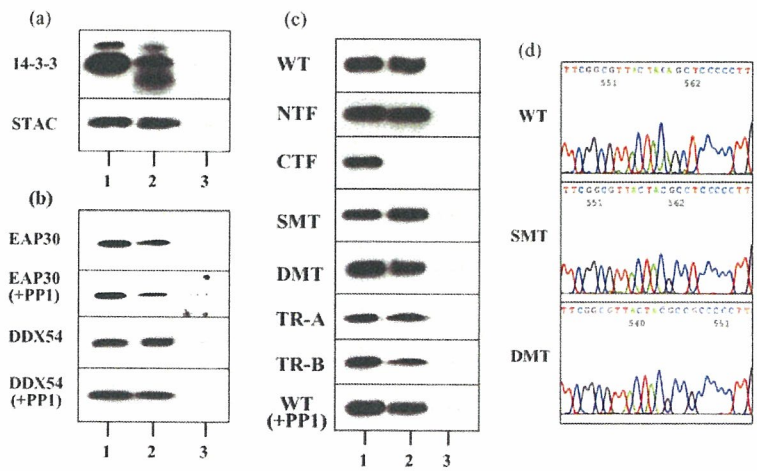

Fig. 2. Immunoprecipitation analysis of 14-3-3-binding proteins. (a) Binding of STAC to 14-3-3. Total protein extract of HEK293 cells expressing Xpress-tagged recombinant STAC was processed for immunoprecipitation (IP) with rabbit polyclonal antibody reacting with all 14-3-3 isoforms (K-19) or with normal rabbit IgG. The immunoprecipitates were then processed for Western blot analysis using mouse monoclonal antibody reacting with all 14-3-3 isoforms (H-8) (upper panel) or mouse monoclonal anti-Xpress antibody (lower panel). Lanes (1–3) represent (1) the input control, and IP with (2) K-19 and (3) normal rabbit IgG. (b) Binding of EAP30 and DDX54 to 14-3-3. Total protein of HEK293 cells expressing Xpress-tagged recombinant EAP30 or DDX54 extracted by using the lysis buffer with inclusion of phosphatase inhibitors or with inclusion of protein phosphatase-1 (PP1) instead of phosphatase inhibitors (+PP1) was processed for IP with K-19 or with normal rabbit IgG. The immunoprecipitates were then processed for Western blot analysis using anti-Xpress antibody. Lanes (1–3) represent (1) the input control, and IP with (2) K-19 and (3) normal rabbit IgG. (c) Binding of mutant and truncated STAC to 14-3-3. Total protein was extracted from HEK293 cells expressing a panel of Xpress-tagged recombinant STAC proteins. They include the full-length wild-type (WT) STAC, the N-terminal half (NTF), the C-terminal half (CTF), the S172A mutant (SMT), the S172A and S173A double mutant (DMT), the truncated form lacking the 14-3-3-binding consensus motif RYYSSP (TR-A), the truncated form lacking the cysteine-rich domain (CRD) (TR-B), and WT STAC isolated by using the lysis buffer with inclusion of PP1 instead of phosphatase inhibitors (WT + PP1). Primers utilized for PCR-based cloning and site-directed mutagenesis are listed in Table 1. The lysate was processed for IP with K-19 or with normal rabbit IgG. The immunoprecipitates were then processed for Western blot analysis using anti-Xpress antibody. Lanes (1–3) represent (1) the input control, and IP with (2) K-19 and (3) normal rabbit IgG. (d) The sequence of the 14-3-3-binding consensus motif located in amino acid residues 169-174 in expression vectors of STAC. The panels indicate WT (nucleotide sequence CGT-TAC-TAC-AGC-TCC-CCC: the corresponding amino acid sequence RYYSSP), SMT (CGT-TAC-TAC-GCC-TCC-CCC: RYYASP), and DMT (CGT-TAC-TAC-GCC-GCC-CCC: RYYAAP).

with a single amino acid substitution S172A (the single mutant; SMT) or with double amino acid substitutions S172A and S173A (the double mutant; DMT), the pcDNA4/HisMax-TOPO vector containing the wild-type (WT) STAC gene was modified by consecutive site-directed mutagenesis using QuikChange II site-directed mutagenesis kit (Stratagene) and the primer sets listed in Table 1. The mutations introduced in the vector were verified by sequencing analysis (Fig. 2d). All these vectors were transfected in HEK293 cells by Lipofectamine 2000 reagent.

2.4. Immunoprecipitation analysis

To prepare total protein extract, the cells were homogenized and incubated at room temperature for 30 min in M-PER lysis buffer (Pierce, Rockford, IL) supplemented with a cocktail of protease inhibitors (Sigma), with inclusion of phosphatase inhibitors (Sigma) to maintain the protein phosphorylation status or with inclusion of recombinant protein phosphatase-1 (PP1) catalytic subunit α-isoform (5 U/ml; Sigma) instead of phosphatase inhibitors to induce the protein dephosphorylation reaction (Ichimura et al., 2005), followed by centrifugation at 12,000 rpm at 4 °C for 20 min. After preclearance, the supernatant was incubated at 4 °C for 3 h with 30 μg/ml rabbit polyclonal anti-14-3-3 protein antibody (K19)-conjugated agarose (Santa Cruz Biotechnology, Santa Cruz, CA) or the same amount of normal rabbit IgG-conjugated agarose (Santa Cruz Biotechnology). After several washes, the immunoprecipitates were processed for Western blot analysis using mouse monoclonal anti-14-3-3 protein antibody (H-8, Santa Cruz Biotechnology) and mouse monoclonal anti-Xpress antibody (Invitrogen). K-19 and H-8 antibodies recognize all 14-3-3 isoforms. The specific reaction was visualized using a chemiluminescent substrate (Pierce).

3. Results

3.1. Protein microarray analysis identified 20 distinct 14-3-3-binding partners

To analyze a high-density human protein microarray, the recombinant 14-3-3ε protein tagged with V5 was purified form the supernatant of 293 eV5 cells secreting the recombinant protein in the culture medium. Western blot analysis verified the purity and specificity of the probe (Fig. 1b). Among 1752 proteins on the microarray, 20 were identified as the proteins showing significant binding to the probe (Table 2). All of these were previously unreported 14-3-3-binding partners by the BIND search. Seven were hypothetical clones of uncharacterized function, derived from the mammalian genome collection (MGC) or the full-length long Japan (FLJ). Thirteen annotated proteins included EAP30 subunit of ELL complex (EAP30) (Fig. 1d), lymphocyte cytosolic protein 2 (LCP2), methionine aminopeptidase 2 (METAP2), melanoma antigen family B, 4 (MAGEB4), chondroitin 4 sulfotransferase 11 (CHST11), nuclear interacting partner of anaplastic lymphoma kinase (ZC3HC1), minichromosome maintenance deficient 10 (MCM10), DEAD box polypeptide 54 (DDX54) (Fig. 1e), heterogeneous nuclear ribonucleoprotein C (HNPRC), fibroblast growth factor 12 (FGF12), glutathione *S*-transferase M3 (GSTM3), src homology three (SH3) and cysteine rich domain (STAC) (Fig. 1f), and ATPase, H+ transporting, lysosomal, 21 kDa, V0 subunit C″ (ATP6V0B). The 14-3-3-binding consensus motif mode I (RSX*p*SXP) was found only in STAC (*pS*172) and HNRPC (*pS*125) by the Scansite Motif Scanner search under the high stringent condition, while 15 of 20 proteins have one or several motifs when a query with the medium or low stringency was performed (Table 2).

3.2. Immunoprecipitation analysis validated the specific binding to 14-3-3

EAP30, DDX54, and STAC were selected to verify the results of microarray analysis, in view of their higher Z-scores. The recombinant proteins were expressed in HEK293 cells, which constitutively express a substantial amount of endogenous 14-3-3 protein. Total protein was extracted by using the lysis buffer with inclusion of phosphatase inhibitors to maintain the protein phosphorylation status or with inclusion of recombinant protein phosphatase-1 (PP1) instead of phosphatase inhibitors to induce the protein dephosphorylation reaction, followed by processing for immunoprecipitation (IP) with rabbit polyclonal antibody reacting with all 14-3-3 isoforms (K-19) or with normal rabbit IgG. K19 coimmunoprecipitated 14-3-3 and STAC from the lysate of HEK293 cells expressing the recombinant STAC protein, whereas normal rabbit IgG did not pull down these proteins (Fig. 2a). K-19 immunoprecipitated EAP30 and DDX54 from the lysate of HEK293 cells expressing the recombinant EAP30 or DDX54 protein, respectively, under both phosphorylated and dephosphorylated conditions (Fig. 2b). These results indicate that EAP30, DDX54, and STAC could interact with the endogenous 14-3-3 protein in HEK293 cells where the corresponding recombinant proteins were expressed.

STAC has the highly stringent 14-3-3-binding consensus motif RYYSSP in amino acid residues 169-174 (*pS*172), as suggested by the Scansite Motif Scanner (Table 2). Therefore, a possible involvement of this motif in binding to 14-3-3 was investigated by IP analysis of a series of mutant and truncated STAC proteins (Table 1). K-19 immunoprecipitated the full-length wild-type (WT) STAC comprised of amino acid residues 2-402 (Fig. 2a and c). K-19 also pulled down the S172A mutant (SMT), and the S172A and S173A double mutant (DMT), and the N-terminal half (NTF; amino acid residues 2-233) from the lysate of HEK293 cells expressing the corresponding recombinant proteins (Fig. 2c). In contrast, K-19 did not pull down the C-terminal half (CTF; amino acid residues 234-402) (Fig. 2c). These observations indicate that the RYYSSP motif is not essential for binding of STAC to 14-3-3. This was confirmed by the observations that K-19 immunoprecipitated the truncated form lacking the RYYSSP sequence (TR-A; amino acid residues 2-164) and the shortest form lacking both the RYYSSP sequence and the cysteine-rich domain (CRD) (TR-B; amino acid residues 2-105) from the lysate of HEK293 cells expressing the corresponding recombinant proteins (Fig. 2c). Finally, the full-length WT STAC interacted with 14-3-3 under the dephosphorylated condition (Fig. 2c). These observations indicate that the

Table 2
Twenty 14-3-3-binding proteins identified by protein microarray analysis

No.	Symbol	Database ID	Protein name	Putative biological function	14-3-3-binding consensus motif mode I	Stringency level of the binding motif	Subarray	Row	Column	Z-score
1	EAP30	NM_007241	EAP30 subunit of ELL complex	a 30-kDa component of the ELL complex that confers derepression of transcription by RNA polymerase II	No sites	NA	1	7	11	22.8593
									12	24.60829
2	FLJ10415	NM_018089	Hypothetical protein, cDNA clone MGC:969	Unknown	S258: ARGGPSHSAGANLRR	Low	5	4	11	4.16265
					S405: SPKQGSGSEGEDGFQ	Low			12	4.35203
					S525: PADPRVLSLLSAPLG	Low				
					S690: VNTRRCWSCGASLQG	Low				
3	LOC57228	NM_020467	Hypothetical protein	Unknown	S28: AARKRNISSNDSQAP	Low	5	6	9	16.84741
									10	17.1519
4	MGC17403	NM_152634	Hypothetical protein	Unknown	T274: KQLRASYTESCIQEH	Low	11	3	1	4.04754
									2	4.08838
5	LCP2	NM_005565	Lymphocyte cytosolic protein 2	A 72-kDa protein (SLP76) that associates with the Grb2 adaptor protein, provides a substrate of the ZAP-70 protein tyrosine kinase, and plays a role in promoting T cell development and activation	S297: TTERHERSSPLPGKK	Low	13	5	11	4.47457
					S376: SSFPQSASLPPYFSQ	Low			12	4.46343
					T456: DSSKKTTTNPYVLMV	Low				
6	METAP2	NM_006838	Methionine aminopeptidase 2	A 67-kDa protein that interacts with eukaryotic initiation factor-2 (eIF-2) and regulates protein synthesis	T113: KRGPKVQTDPPSVPI	Low	15	6	11	3.54252
					S152: TAAWRTTSEEKKALD	Low			12	3.31601
7	MAGEB4	NM_002367	Melanoma antigen family B, 4	A member of the MAGEB family expressed in testis whose function remains unknown	T18: AREKRQRTRGQTQDL	Medium	18	3	7	9.50614
					T194: GNQSSAWTLPRNGLL	Low			8	9.30562
					S339: SAYSRATSSSSSQPM	Low				
8	CHST11	NM_018413	Chondroitin 4 sulfotransferase 11	A member of HNK-1ST family GalNAc 4-O-sulfotransferase that plays a role in chondroitin sulfate and dermatan sulfate biosynthesis	S93: TDTCRANSATSRKRR	Medium	20	5	3	3.97327
					S56: DICCRKGSRSPLQEL	Low			4	3.92871
					S194: EPFERLVSAYRNKFT	Low				
9	ZC3HC1	NM_016478	Nuclear interacting partner of anaplastic lymphoma kinase (ALK)	A 60-kDa protein that interacts with ALK and plays an antiapoptotic role in nucleophosmin-ALK signaling events	No sites	NA	23	3	3	3.33458
									4	3.55366

Table 2 (*Continued*)

No.	Symbol	Database ID	Protein name	Putative biological function	14-3-3-binding consensus motif mode I	Stringency level of the binding motif	Subarray	Row	Column	Z-score
10	MCM10	NM_018518	Minichromosome maintenance deficient 10	A key component of the pre-replication complex (pre-RC) that is essential for the initiation of DNA replication	S90: AQPPRTGSEFPRLEG	Medium	25	3	13	4.26291
					S35: KPAIKSISASALLKQ	Low			14	4.12552
					S55: LEMRRRKSEEIQKRF	Low				
					S302: PCGNRSISLDRLPNK	Low				
					T329: DGMLKEKTGPKIGGE	Low				
11	DDX54	NM_024072	DEAD (Asp-Glu-Ala-Asp) box polypeptide 54	A 97-kDa RNA helicase (DP97) that interacts with estrogen receptor (ER) and represses the transcription of ER-regulated genes	T95: EDKKKIKTESGRYIS	Low	27	3	15	9.2425
					S102: TESGRYISSSYKRDL	Low			16	9.10882
12	HNPRC	NM_004500	Heterogeneous nuclear ribonucleoprotein C	A member of heterogeneous nuclear ribonucleoproteins (hnRNPs) involved in pre-mRNA processing, mRNA metabolism and transport	S125: DYYDRMYSYPARVPP	High	28	6	9	4.81248
					S158: NTSRRGKSGFNSKSG	Low			10	5.18382
					S170: KSGQRGSSKSGKLKG	Low				
					S240: ETNVKMESEGGADDS	Low				
13	LOC137781	BC032347	Hypothetical gene, cDNA clone MGC:40429	Unknown	No sites	NA	30	5	11	3.56109
									12	3.47568
14	LOC92345	NM_138386	Hypothetical protein	Unknown	S339: QGRKKLKSEFNEPGE	Low	32	5	13	3.55366
					T374: GYRNREFTRGFSRAR	Low			14	3.73933
					S467: PLLNLPYSLPPPPPP	Low				
15	FGF12	NM_004113	Fibroblast growth factor 12, transcript variant 2	A member of the FGF family that plays a role in nervous system development and function	S150: VCMYREQSLHEIGEK	Low	34	6	5	5.73339
					S165: QGRSRKSSGTPTMNG	Low			6	5.75567
16	GSTM3	NM_000849	Glutathione *S*-transferase M3 (brain)	A cytoplasmic glutathione *S*-transferase of the mu class that plays a role in detoxification of carcinogens, therapeutic drugs, environmental toxins, and products of oxidative stress	S64: GIKLRSFSV	Low	38	5	15	7.82029
									16	7.70889
17	STAC	NM_003149	src homology three (SH3) and cysteine rich domain	A 47-kDa protein with a SH3 and a cysteine-rich domain that plays a role in the neuron-specific signal transduction pathway	S172: KGFRRYYSSPLLIHE	High	39	5	1	16.63575
					S56: TKSLRSKSADNFFQR	Medium			2	16.64318
					S255: DLRKRSNSVFTYPEN	Medium				
					S46: QKLKRSLSFKTKSLR	Low				
					S51: SLSFKTKSLRSKSAD	Low				
					S66: NFFQRTNSEDMKLQA	Low				
					S253: GYDLRKRSNSVFTYP	Low				

18	FLJ10156	NM_019013	Hypothetical protein, cDNA clone MGC:961	Unknown	S16: GTSVRRRSLQHQEQL	Low	41	3	7	7.31156
					T190: FRSPYSSTEPLCSPS	Low			8	6.94023
19	ATP6V0B	NM_004047	ATPase, H+ transporting, lysosomal, 21 kD, V0 subunit C″	A 23-kDa component of vacuolar ATPase that mediates acidification of intracellular organelles	No sites	NA	43	7	3	3.3123
									4	3.60565
20	FLJ25758	NM_001011541	Hypothetical protein, clone MGC:33355	Unknown	No sites	NA	48	7	7	4.18864
									8	4.18122

Among 1752 proteins on the microarray, 20 were identified as showing a significant interaction, based on the signal intensity value exceeding the median plus three standard deviations of all the fluorescence intensities by analyzing with ProtoArray Prospector software. They are listed with the 14-3-3-binding consensus motif (putative phosphoserine and phosphothreonine indicated by underline) and its stringency level by the Scansite Motif Scanner, the position on the array, and the *Z*-score calculated as described in Section 2. Abbreviations: FLJ, the full-length long Japan; MGC, mammalian gene collection; NA, not available.

14-3-3-interacting domain is located in the N-terminal segment spanning amino acid residues 2-105 of STAC, and the interaction is independent of serine/threonine-phosphorylation of the binding domain of STAC.

4. Discussion

The present study was designed to rapidly and systematically identify 14-3-3-binding proteins by analyzing a high-density protein microarray. The array included 1752 proteins derived from multiple gene families of biological importance, including cell-signaling proteins, kinases, membrane-associated proteins, and metabolic proteins. In general, protein microarray has its own limitations associated with the expression and purification of a wide variety of target proteins. In the microarray we utilized, the target proteins were expressed in a baculovirus expression system, purified under native conditions, and spotted on the slides to ensure the preservation of native structure, posttranslational modifications, including glycosylation and serine phophorylation (Culleré et al., 1998; Tennagels et al., 1999), and proper functionality. Immunolabeling of the array with anti-phosphotyrosine (pTyr) antibody indicated that approximately 10–20% of the proteins on the array are phosphorylated (the unpublished data of Invitrogen Technical Service). When this microarray was utilized for kinase substrate identification, most of known kinases immobilized on the array are enzymatically active with the capacity of some degree of autophosphorylation, suggesting that they are certainly phosphorylated on tyrosine, serine, and threonine residues (see the Protoarray application note on http://www.invitrogen.com/protoarray). However, we could not currently validate the precise levels of phosphorylation of individual proteins, because of a lack of anti-phosphoserine (pSer) and anti-phosphothreonine (pThr) antibodies suitable for detection of pSer and pThr residues of the proteins on glass slide.

The protein microarray utilized in the present study includes 11 known 14-3-3-binding proteins, such as PCTAIRE protein kinase 1 (PCTK1) (Graeser et al., 2002), protein kinase C zeta (PRKCZ) (van der Hoeven et al., 2000), keratin 18 (KRT18) (Ku et al., 1998), myosin light polypeptide kinase (MYLK) (Haydon et al., 2002), v-abl Abelson murine leukemia viral oncogene homolog 1 (ABL1) (Yoshida et al., 2005), v-akt murine thymoma viral oncogene homolog 1 (AKT1) (Powell et al., 2002), epidermal growth factor receptor (EGFR) (Oksvold et al., 2004), cell division cycle 2 (CDC2) (Chan et al., 1999), mitogen-activated protein kinase kinase kinase 1 (MAP3K1) (Fanger et al., 1998), mitogen-activated protein kinase-activated protein kinase 2 (MAPKAPK2) (Powell et al., 2003), and stratifin (SFN) (Benzinger et al., 2005) (Table 3). All of these were not identified as a 14-3-3-binding protein in the present study. Therefore, the possibility could not be excluded that some 14-3-3 binding partners were not detected due to imperfect phosphorylation of the proteins on the array or due to 14-3-3 isoform-specific binding. Calmodulin, another known 14-3-3 interactor (Luk et al., 1999), was included as a negative control on the array and identified as negative in the present study, because the calcium-dependent interaction between 14-3-3 and calmodulin could not be detected under the calcium-free conditions we employed.

Table 3
Eleven known 14-3-3-binding proteins immobilized on the protein microarray utilized in the present study

Gene name	Database ID	Reference
PCTAIRE protein kinase 1 (PCTK1), transcript variant 3	NM_033019	Graeser et al. (2002)
Protein kinase C, zeta (PRKCZ)	NM_002744	van der Hoeven et al. (2000)
Keratin 18 (KRT18), transcript variant 1	NM_000224	Ku et al. (1998)
Myosin, light polypeptide kinase (MYLK), transcript variant 6	NM_005965	Haydon et al. (2002)
V-abl Abelson murine leukemia viral oncogene homolog 1 (ABL1), transcript variant a	NM_005157	Yoshida et al. (2005)
V-akt murine thymoma viral oncogene homolog 1 (AKT1), transcript variant 1	NM_005163	Powell et al. (2002)
Epidermal growth factor receptor (EGFR), transcript variant 1	NM_005228	Oksvold et al. (2004)
Cell division cycle 2 (CDC2), transcript variant 1	NM_001786	Chan et al. (1999)
Mitogen-activated protein kinase kinase kinase 1 (MAP3K1)	XM_042066	Fanger et al. (1998)
Mitogen-activated protein kinase-activated protein kinase 2 (MAPKAPK2), transcript variant 1	NM_004759	Powell et al. (2003)
14-3-3 Sigma, stratifin (SFN)	NM_006142	Benzinger et al. (2005)

The known 14-3-3-binding proteins, which were spotted on the protein microarray but were not detected in the present study are listed. The 14-3-3-binding proteins validated by definitive evidence are selected and shown with references.

Increasing studies indicate that 14-3-3-binding phosphorylation sites do not exactly fit the consensus motif (Aitken et al., 2002; Ku et al., 1998) and a second site is required to enhance a stable 14-3-3-target interaction (MacKintosh, 2004), and show that the 14-3-3 protein interacts with a set of target proteins in a phosphorylation-independent manner (Dai and Murakami, 2003; Henriksson et al., 2002; Zhai et al., 2001). Supporting the latter possibility, the present observations showed that the interaction of 14-3-3 with target proteins is independent of serine/threonine-phosphorylation of the binding sites of EAP30, DDX54, and STAC. This suggests that substantial numbers of 14-3-3 binding partners identified by protein microarray analysis, if not all, employ phosphorylation-independent binding domains.

All the procedure required for microarray analysis takes approximately 5 h. This analysis identified a set of 20 human proteins as 14-3-3 interactors, most of which were previously unreported except for glutathione *S*-transferase M3 (GSTM3) that was found as one of binding partners by 14-3-3 affinity purification of HeLa cell protein extracts (Pozuelo Rubio et al., 2004). Unexpectedly, the highly stringent 14-3-3-binding consensus motif was identified only in two, such as STAC and HNPRC, by the Scansite Motif Scanner search, while 15 of 20 proteins have one or several motifs when a query with the medium or low stringency was performed (Table 2). The specific binding to 14-3-3 of EAP30, DDX54, and STAC was verified by immunoprecipitation analysis of the recombinant proteins expressed in HEK293 cells. These results indicate that protein microarray is a powerful tool for rapid identification of protein–protein interactions, including those unpredicted by the Database search.

Among the 14-3-3-binding partners we identified, several proteins could be categorized as a component of multimolecular complexes involved in transcriptional regulation. ELL is a human oncogene encoding a RNA polymerase II (Pol II) transcription factor that promotes transcription elongation (Schmidt et al., 1999). EAP30 is a 30-kDa component of the ELL complex where EAP30 confers derepression of transcription by Pol II (Schmidt et al., 1999). A recent study showed that EAP30 could interact with the tumor susceptibility gene TSG101 product, a cellular factor that plays a key role in packaging of HIV virions (von Schwedler et al., 2003). DDX54 is a 97-kDa RNA helicase (DP97) that interacts with estrogen receptor (ER) and represses the transcription of ER-regulated genes (Rajendran et al., 2003). A recent study by using chromatin immunoprecipitation (ChIP) assay combined with promoter microarray analysis showed that hepatocyte nuclear factor 4-alpha (HNF4α), a master regulator of hepatocyte gene expression, interacts with the DDX54 gene promoter, together with Pol II (Odom et al., 2004). HNPRC is a member of heterogeneous nuclear ribonucleoproteins (hnRNPs) involved in pre-mRNA processing, mRNA metabolism and transport (Nakagawa et al., 1986). Increasing evidence indicates that the 14-3-3 protein and its targets are widely distributed in various subcellular compartments, including the nucleus (Dougherty and Morrison, 2004; Meek et al., 2004).

STAC is a 47-kDa cytosolic protein that has a cysteine-rich domain (CRD) of the protein kinase C family in the N-terminal half (NTF), and a src homology three (SH3) domain in the C-terminal half (CTF), suggesting its function as an adapter on which divergent signaling pathways converge (Hardy et al., 2005; Suzuki et al., 1996). STAC is expressed predominantly in the brain with the distribution in a defined population of neurons (Suzuki et al., 1996). IP analysis of mutant and truncated forms argued against an active involvement of the most stringent motif RYYSSP (*pS*172) of STAC in its binding to 14-3-3. The present observations indicated that the 14-3-3-interacting domain is located in the N-terminal segment spanning amino acid residues 2-105 of STAC and the interaction is serine/threonine phosphorylation-independent.

In conclusion, protein microarray is a useful tool for rapid and comprehensive profiling of 14-3-3-binding proteins, although the validation of the results by different methods is highly important.

Acknowledgements

This work was supported by grants from Research on Psychiatric and Neurological Diseases and Mental Health, the Ministry of Health, Labour and Welfare of Japan (H17-020), Research on Health Sciences Focusing on Drug Innovation, the Japan Health Sciences Foundation (KH21101), the Grant-in-Aid for Scientific

Research, the Ministry of Education, Science, Sports and Culture (B2-15390280 and PA007-16017320), and the Program for Promotion of Fundamental Studies in Health Sciences of the National Institute of Biomedical Innovation (NIBIO), Japan.

Appendix A. Supplementary data

Supplementary data associated with this article can be found, in the online version, at 10.1016/j.jneumeth.2005.09.015.

References

Aitken A, Baxter H, Dubois T, Clokie S, Mackie S, Mitchell K, Peden A, Zemlickova E. 14-3-3 proteins in cell regulation. Biochem Soc Trans 2002;30:351–60.

Benzinger A, Muster N, Koch HB, Yates 3rd JR, Hermeking H. Targeted proteomic analysis of 14-3-3 sigma, a p53 effector commonly silenced in cancer. Mol Cell Proteomics 2005;4:785–95.

Berg D, Holzmann C, Riess O. 14-3-3 proteins in the nervous system. Nat Rev Neurosci 2002;4:752–62.

Chan SM, Ermann J, Su L, Fathman CG, Utz PJ. Protein microarrays for multiplex analysis of signal transduction pathways. Nat Med 2004;10:1390–6.

Chan TA, Hermeking H, Lengauer C, Kinzler KW, Vogelstein B. 14-3-3σ is required to prevent mitotic catastrophe after DNA damage. Nature 1999;401:616–20.

Chen H-K, Fernandez-Funez P, Acevedo SF, Lam YC, Kaytor MD, Fernandez MH, Aitken A, Skoulakis EM, Orr HT, Botas J, Zoghbi HY. Interaction of Akt-phosphorylated ataxin-1 with 14-3-3 mediates neurodegeneration in spinocerebellar ataxia type 1. Cell 2003;113:457–68.

Culleré X, Rose P, Thathamangalam U, Chatterjee A, Mullane KP, Pallas DC, Benjamin TL, Roberts TM, Schaffhausen BS. Serine 257 phosphorylation regulates association of polyomavirus middle T antigen with 14-3-3 proteins. J Virol 1998;72:558–63.

Dai J-G, Murakami K. Constitutively and autonomously active protein kinase C associated with 14-3-3 ζ in the rodent brain. J Neurochem 2003;84:23–34.

Dougherty MK, Morrison DK. Unlocking the code of 14-3-3. J Cell Sci 2004;117:1875–84.

Fanger GR, Widmann C, Porter AC, Sather S, Johnson GL, Vaillancourt RR. 14-3-3 proteins interact with specific MEK kinases. J Biol Chem 1998;273:3476–83.

Fu H, Subramanian RR, Masters SC. 14-3-3 proteins: structure, function, and regulation. Annu Rev Pharmacol Toxicol 2000;40:617–47.

Graeser R, Gannon J, Poon RYC, Dubois T, Aitken A, Hunt T. Regulation of the CDK-related protein kinase PCTAIRE-1 and its possible role in neurite outgrowth in Neuro-2A cells. J Cell Sci 2002;115:3479–90.

Hardy K, Mansfield L, Mackay A, Benvenuti S, Ismail S, Arora P, O'Hare MJ, Jat PS. Transcriptional networks and cellular senescence in human mammary fibroblasts. Mol Biol Cell 2005;16:943–53.

Haydon CE, Watt PW, Morrice N, Knebel A, Gaestel M, Cohen P. Identification of a phosphorylation site on skeletal muscle myosin light chain kinase that becomes phosphorylated during muscle contraction. Arch Biochem Biophys 2002;397:224–31.

Henriksson ML, Francis MS, Peden A, Aili M, Stefansson K, Palmer R, Aitken A, Hallberg B. A nonphosphorylated 14-3-3 binding motif on exoenzyme S that is functional in vivo. Eur J Biochem 2002;269:4921–9.

Ichimura T, Yamamura H, Sasamoto K, Tominaga Y, Taoka M, Kakiuchi K, Shinkawa T, Takahashi N, Shimada S, Isobe T. 14-3-3 proteins modulate the expression of epithelial Na^+ channels by phosphorylation-dependent interaction with Nedd4-2 ubiquitin ligase. J Biol Chem 2005;280:13187–94.

Jin J, Smith FD, Stark C, Wells CD, Fawcett JP, Kulkarni S, Metalnikov P, O'Donnell P, Taylor P, Taylor L, Zougman A, Woodgett JR, Langeberg LK, Scott JD, Pawson T. Proteomic, functional, and domain-based analysis of in vivo 14-3-3 binding proteins involved in cytoskeletal regulation and cellular oraganization. Curr Biol 2004;14:1436–50.

Kawamoto Y, Akiguchi I, Nakamura S, Honjyo Y, Shibasaki H, Budka H. 14-3-3 proteins in Lewy bodies in Parkinson disease and diffuse Lewy body disease brains. J Neuropathol Exp Neurol 2002;61:245–53.

Ku N-O, Liao J, Omary MB. Phosphorylation of human keratin 18 serine 33 regulates binding to 14-3-3 proteins. EMBO J 1998;17:1892–906.

Layfield R, Fergusson J, Aitken A, Lowe J, Landon M, Mayer RJ. Neurofibrillary tangles of Alzheimer's disease brains contain 14-3-3 proteins. Neurosci Lett 1996;209:57–60.

Luk SCW, Ngai S-M, Tsui SKW, Fung K-P, Lee C-Y, Waye MMY. In vivo and in vitro association of 14-3-3 epsilon isoform with calmodulin: implication for signal transduction and cell proliferation. J Cell Biochem 1999;73:31–5.

MacBeath G, Schreiber SL. Printing proteins as microarrays for high-throughput function determination. Science 2000;289:1760–3.

MacKintosh C. Dynamic interactions between 14-3-3 proteins and phosphoproteins regulate diverse cellular processes. Biochem J 2004;381:329–42.

Malaspina A, Kaushik N, de Belleroche J. A 14-3-3 mRNA is up-regulated in amyotrophic lateral sclerosis spinal cord. J Neurochem 2000;75:2511–20.

Meek SEM, Lane WS, Piwnica-Worms H. Comprehensive proteomic analysis of interphase and mitotic 14-3-3-binding proteins. J Biol Chem 2004;279:32046–54.

Michaud GA, Salcius M, Zhou F, Bangham R, Bonin J, Guo H, Snyder M, Predki PF, Schweitzer BI. Analyzing antibody specificity with whole proteome microarrays. Nat Biotechnol 2003;21:1509–12.

Nakagawa TY, Swanson MS, Wold BJ, Dreyfuss G. Molecular cloning of cDNA for the nuclear ribonucleoprotein particle C proteins: a conserved gene family. Proc Natl Acad Sci USA 1986;83:2007–11.

Obenauer JC, Cantley LC, Yaffe MB. Scansite 2.0: Proteome-wide prediction of cell signaling interactions using short sequence motifs. Nucl Acids Res 2003;31:3635–41.

Odom DT, Zizlsperger N, Gordon DB, Bell GW, Rinaldi NJ, Murray HL, Volkert TL, Schreiber J, Rolfe PA, Gifford DK, Fraenkel E, Bell GI, Young RA. Control of pancreas and liver gene expression by HNF transcription factors. Science 2004;303:1378–81.

Oksvold MP, Huitfeldt HS, Langdon WY. Identification of 14-3-3ζ as an EGF receptor interacting protein. FEBS Lett 2004;569:207–10.

Pozuelo Rubio M, Geraghty KM, Wong BH, Wood NT, Campbell DG, Morrice N, Mackintosh C. 14-3-3-affinity purification of over 200 human phosphoproteins reveals new links to regulation of cellular metabolism, proliferation and trafficking. Biochem J 2004;379:395–408.

Powell DW, Rane MJ, Chen Q, Singh S, McLeish KR. Identification of 14-3-3ζ as a protein kinase B/Akt substrate. J Biol Chem 2002;277:21639–42.

Powell DW, Rane MJ, Joughin BA, Kalmukova R, Hong J-H, Tidor B, Dean WL, Pierce WM, Klein JB, Yaffe MB, McLeish KR. Proteomic identification of 14-3-3ζ as a mitogen-activated protein kinase-activated protein kinase 2 substrate: role in dimmer formation and ligand binding. Mol Cell Biol 2003;23:5376–87.

Rajendran RR, Nye AC, Frasor J, Balsara RD, Martini PG, Katzenellenbogen BS. Regulation of nuclear receptor transcriptional activity by a novel DEAD box RNA helicase (DP97). J Biol Chem 2003;278:4628–38.

Satoh J, Kuroda Y. Differential gene expression between human neurons and neuronal progenitor cells in culture: an analysis of arrayed cDNA clones in NTera2 human embryonal carcinoma cell line as a model system. J Neurosci Meth 2000;94:155–64.

Satoh J, Yamamura T. Gene expression profile following stable expression of the cellular prion protein. Cell Mol Neurobiol 2004;24:793–814.

Satoh J, Yamamura T, Arima K. The 14-3-3 protein ε isoform expressed in reactive astrocytes in demyelinating lesions of multiple sclerosis binds to vimentin and glial fibrillary acidic protein in cultured human astrocytes. Am J Pathol 2004;165:577–92.

Schmidt AE, Miller T, Schmidt SL, Shiekhattar R, Shilatifard A. Cloning and characterization of the EAP30 subunit of the ELL complex that confers derepression of transcription by RNA polymerase II. J Biol Chem 1999;274:21981–5.

Suzuki H, Kawai J, Taga C, Yaoi T, Hara A, Hirose K, Hayashizaki Y, Watanabe S. Stac, a novel neuron-specific protein with cysteine-rich and SH3 domains. Biochem Biophys Res Commun 1996;229:902–9.

Tennagels N, Hube-Magg C, Wirth A, Noelle V, Klein HW. Expression, purification, and characterization of the cytoplasmic domain of the human IGF-1 receptor using a baculovirus expression system. Biochem Biophys Res Commun 1999;260:724–8.

van der Hoeven PCJ, van der Wal JCM, Ruurs P, van Blitterswijk WJ. Protein kinase C activation by acidic proteins including 14-3-3. Biochem J 2000;347:781–5.

van Hemert MJ, Steensma HY, van Heusden GPH. 14-3-3 proteins: key regulators of cell division, signaling and apoptosis. Bioessays 2001;23:936–47.

Vidalain PO, Boxem M, Ge H, Li S, Vidal M. Increasing specificity in high-throughput yeast two-hybrid experiments. Methods 2004;32:363–70.

von Mering C, Krause R, Snel B, Cornell M, Oliver SG, Fields S, Bork P. Comparative assessment of large-scale data sets of protein–protein interactions. Nature 2002;417:399–403.

von Schwedler UK, Stuchell M, Müller B, Ward DM, Chung HY, Morita E, Wang HE, Davis T, He GP, Cimbora DM, Scott A, Kräusslich HG, Kaplan J, Morham SG, Sundquist WI. The protein network of HIV budding. Cell 2003;114:701–13.

Yoshida K, Yamaguchi T, Natsume T, Kufe D, Miki Y. JNK phosphorylation of 14-3-3 proteins regulates nuclear targeting of c-Abl in the apoptotic response to DNA damage. Nat Cell Biol 2005;7:278–85.

Zerr I, Bodemer M, Gefeller O, Otto M, Poser S, Wiltfang J, Windl O, Kretzschmar HA, Weber T. Detection of 14-3-3 protein in the cerebrospinal fluid supports the diagnosis of Creutzfeldt–Jakob disease. Ann Neurol 1998;43:32–40.

Zhai J, Lin H, Shamim M, Schlaepfer WW, Cañete-Soler R. Identification of a novel interaction of 14-3-3 with p190RhoGEF. J Biol Chem 2001;276:41318–24.

Zhang LV, Wong SL, King OD, Roth FP. Predicting co-complexed protein pairs using genomic and proteomic data integration. BMC Bioinformat 2004;5:38–52.

Zhu H, Bilgin M, Bangham R, Hall D, Casamayor A, Bertone P, Lan N, Jansen R, Bidlingmaier S, Houfek T, Mitchell T, Miller P, Dean RA, Gerstein M, Snyder M. Global analysis of protein activities using proteome chips. Science 2001;293:2101–5.

ELSEVIER

Journal of Neuroimmunology 174 (2006) 108 – 118

Journal of
Neuroimmunology

www.elsevier.com/locate/jneuroim

T cell gene expression profiling identifies distinct subgroups of Japanese multiple sclerosis patients

Jun-ichi Satoh [a], Megumi Nakanishi [a], Fumiko Koike [a], Hiroyuki Onoue [a], Toshimasa Aranami [a], Toshiyuki Yamamoto [b], Mitsuru Kawai [b], Seiji Kikuchi [c], Kyouichi Nomura [d], Kazumasa Yokoyama [e], Kohei Ota [f], Toshiro Saito [g], Masayuki Ohta [g], Sachiko Miyake [a], Takashi Kanda [h], Toshiyuki Fukazawa [i], Takashi Yamamura [a,*]

[a] *Department of Immunology, National Institute of Neuroscience, NCNP, 4-1-1 Ogawahigashi, Kodaira, Tokyo 187-8502, Japan*
[b] *National Center Hospital for Mental, Nervous and Muscular Disorders, NCNP, Tokyo 187-8502, Japan*
[c] *Department of Neurology, Hokkaido University Graduate School of Medicine, Sapporo 060-8638, Japan*
[d] *Department of Neurology, Saitama Medical School, Saitama 350-0495, Japan*
[e] *Department of Neurology, Juntendo University School of Medicine, Tokyo 113-841, Japan*
[f] *Department of Neurology, Tokyo Women's Medical University, Tokyo 162-8666, Japan*
[g] *Life Science Group, Hitachi Ltd., Saitama 350-1165, Japan*
[h] *Department of Neurology, Tokyo Medical and Dental University, Tokyo 113-8519, Japan*
[i] *Hokuyukai Neurology Hospital, Sapporo 063-0802, Japan*

Received 29 November 2005; received in revised form 30 January 2006; accepted 3 February 2006

Abstract

To clarify the molecular background underlying the heterogeneity of multiple sclerosis (MS), we characterized the gene expression profile of peripheral blood $CD3^+$ T cells isolated from MS and healthy control (CN) subjects by using a cDNA microarray. Among 1258 cDNAs on the array, 286 genes were expressed differentially between 72 untreated Japanese MS patients and 22 age- and sex-matched CN subjects. When this set was used as a discriminator for hierarchical clustering analysis, it identified four distinct subgroups of MS patients and five gene clusters differentially expressed among the subgroups. One of these gene clusters was overexpressed in MS versus CN, and particularly enhanced in the clinically most active subgroup of MS. After 46 of the MS patients were treated with interferon-beta (IFNβ-1b) for two years, IFNβ responders were clustered in two of the four MS subgroups. Furthermore, the IFNβ responders differed from nonresponders in the kinetics of IFN-responsive genes at 3 and 6 months after starting IFNβ treatment. These results suggest that T-cell gene expression profiling is valuable to identify distinct subgroups of MS associated with differential disease activity and therapeutic response to IFNβ.

Keywords: Gene expression profile; Hierarchical clustering analysis; IFNβ responder; Microarray; Multiple sclerosis; T cells

1. Introduction

Multiple sclerosis (MS) is an inflammatory demyelinating disease of the central nervous system (CNS) white matter mediated by an autoimmune process whose development is triggered by a complex interplay of both genetic and environmental factors (Compston and Coles, 2002). Intravenous administration of interferon-gamma (IFNγ) to MS patients in a previous clinical trial provoked acute relapses accompanied by activation of the systemic immune response, indicating a central role of proinflammatory T helper type 1 (Th1) lymphocytes in the immunopathogenesis of MS (Panitch et al., 1987). In contrast, treatment with interferon-beta (IFNβ) produced a

* Corresponding author. Tel.: +81 42 346 1723; fax: +81 42 346 1753.
E-mail address: yamamura@ncnp.go.jp (T. Yamamura).

0165-5728/$ - see front matter © 2006 Elsevier B.V. All rights reserved.
doi:10.1016/j.jneuroim.2006.02.004

beneficial effect on MS patients with a reduction of the relapse rate by approximately 30% (The IFNB Multiple Sclerosis Study Group, 1993; Jacobs et al., 1996; Saida et al., 2005). Recent studies indicated that an early initiation of IFNβ delays the conversion to clinically definite MS in the patients who experienced a first demyelinating event (Jacobs et al., 2000).

MS exhibits a great range of phenotypic variability. It is classified into relapsing–remitting MS (RRMS), secondary progressive MS (SPMS), or primary progressive MS (PPMS) with respect to the disease course, conventional MS (CMS) or opticospinal MS (OSMS) in terms of the lesion distribution (Saida et al., 2005), and IFNβ responder or nonresponder based on the therapeutic response to IFNβ (Waubant et al., 2003). MS brain lesions show a remarkable heterogeneity in the degree of inflammation, complement activation, antibody deposition, demyelination and remyelination, oligodendrocyte apoptosis, and axonal degeneration (Lucchinetti et al., 2000). These observations suggest that MS is a kind of neurological syndrome caused by different immunopathological mechanisms leading to the final common pathway that provokes inflammatory demyelination. Therefore, it is not surprising to find that individual MS patients show highly variable responses to IFNβ treatment. Currently, very little is known about the molecular background underlying clinical and pathological heterogeneity of MS.

DNA microarray technology is a novel approach that allows us to systematically monitor the expression of a large number of genes in disease-affected tissues (Staudt, 2001). This approach has discovered therapeutically relevant targets and prognostic markers for cancers (Alizadeh et al., 2000; van de Vijver et al., 2000), and has given new insights into the complexity of molecular interactions promoting the autoimmune process in MS (Steinman and Zamvil, 2003). Importantly, the comprehensive gene expression profiling of MS brain tissues and peripheral blood lymphocytes identified a battery of genes deregulated in MS, whose role has not been previously predicted in its pathogenesis (Lock et al., 2002; Graumann et al., 2003; Tajouri et al., 2003; Stürzbecher et al., 2003; Achiron et al., 2004). However, most of previous studies have focused on gene expression in heterogeneous populations of unfractionated lymphocytes and brain cells. Recently, by using microarray we showed that IFNβ treatment elevates the expression of 7 IFN-responsive genes in highly purified peripheral blood $CD3^+$ T cells of 13 Japanese RRMS patients (Koike et al., 2003). More recently, we found that the majority of differentially expressed genes in $CD3^+$ T cells between 72 untreated MS patients and 22 healthy control (CN) subjects were categorized into apoptosis signaling-related genes (Satoh et al., 2005).

To extend our previous studies, we conducted hierarchical clustering analysis of differentially expressed genes between MS and CN in peripheral blood $CD3^+$ T cells. Here we report that T-cell gene expression profiling classifies a heterogeneous population of Japanese MS into four subgroups that differ in the disease activity and therapeutic response to IFNβ, suggesting that this analysis could be applied for designing tailor-made treatment of MS.

2. Subjects and methods

2.1. The study population

The Research Group for IFNβ treatment of Japanese MS, sponsored by the Ministry of Health, Labour and Welfare of Japan, conducted the present study. It enrolled 72 clinically active Japanese MS patients, including 65 RRMS and 7 SPMS cases composed of 55 women and 17 men with the mean age of 36.1±10.3 years, and 22 healthy control (CN) subjects composed of 16 women and 6 men with the mean age of 38.6±12.3 years. The members of this research group (SK, KN, KY, KO, TK, TF and TY), all of who are certified neurologists, diagnosed individual cases according to the established criteria (McDonald et al., 2001), and followed up the patients for at least two years after entry. The patients showed the mean Expanded Disability Status Scale (EDSS) score of 2.8±2.0 upon entry. No patients had a history of treatment with interferons, glatiramer acetate or mitoxantrone before enrollment, or received corticosteroids and other immunosuppressants during at least one month before blood sampling. MS patients were divided into two groups according to their own determination upon entry: one treated with IFNβ and the other without IFNβ. The IFNβ-treated group included 46 patients who started to receive an administration of 8 million units of IFNβ-1b (Betaferon, Schering, Osaka, Japan) for two years given subcutaneously on alternate days, while the IFNβ-untreated group included 26 patients who were followed up without IFNβ treatment for successive two years. From the IFNβ-treated group, blood samples were taken at three time points: before starting IFNβ treatment (designated Pre) and at 3 and 6 months after starting the treatment. In the IFNβ-untreated group, they were collected twice: at enrollment and at 6 months after the enrollment. In case of acute relapse, the patients in both groups were given intravenous methylprednisolone pulse (IVMP) following the standard protocol, although none received glatiramer acetate, mitoxantrone, or other immunosuppressants. The samples obtained during clinically obvious relapses or episodes of infection were omitted. Written informed consent was obtained from all the subjects. The present study was approved by the Ethics Committee of National Center of Neurology and Psychiatry (NCNP).

2.2. IFN β responder/nonresponder score

To evaluate the therapeutic response to IFNβ, we monitored the following six parameters during four years spanning two years before and after initiation of IFNβ

treatment; the number of clinical relapse, the day of IVMP treatment, the day of hospitalization, EDSS score, the number of lesions on T2-weighted MRI, and the patient's satisfaction on the treatment (Table 1). When compared before and after IFNβ treatment, these parameters have given three ranks and scores; good (+1), intermediate (0), and poor (−1). The total score was calculated for each patient, ranging from the maximum value of +6 to the minimum value of −6. The patients with the total score equal to or greater than +3 were considered as being the responder (R), the score from 0 to +2 as one with the undetermined response (UD), and the score equal to or smaller than −1 as the nonresponder (NR) (Table 1).

2.3. cDNA microarray analysis

The present study utilized a custom microarray containing duplicate spots of 1258 cDNA immobilized on a poly-L-lysine-coated slide glass. They were composed of well annotated genes of various functional classes, including cytokines/growth factors and their receptors, apoptosis regulators, oncogenes, transcription factors, signal transducers, cell cycle regulators and housekeeping genes (Hitachi Life Science, Kawagoe, Saitama, Japan; http://www.hitachi.co.jp/LS). Peripheral blood mononuclear cells (PBMC) were isolated from 30 ml of heparinized blood by centrifugation on a Ficoll density gradient. They were labeled with anti-CD3 antibody-coated magnetic microbeads (#130-050-101, Miltenyi Biotec, Auburn, CA), and $CD3^+$ T cells were separated by AutoMACS (Miltenyi Biotec). The remaining cells after the positive selection of $CD3^+$ T cells were harvested as $CD3^-$ non-T cell fraction as described previously (Koike et al., 2003; Satoh et al., 2005). Total RNA was isolated from the cells by using RNeasy Mini Kit (Qiagen, Valencia, CA). Five micrograms of purified RNA was in vitro amplified, and the antisense RNA (aRNA) of MS patients and CN subjects was labeled with a fluorescent dye Cy5, while pooled aRNA of three independent healthy volunteers who were not included in the present study was labeled with Cy3 for a universal reference to standardize the gene expression levels throughout the experiments. The arrays were hybridized at 62 °C for 10 h in the hybridization buffer containing equal amounts of Cy3- or Cy5-labeled cDNA, and they were then scanned by the ScanArray 5000 scanner (GSI Lumonics, Boston, MA). The data were analyzed by using the QuantArray software (GSI Lumonics). The average of fluorescence intensities (FI) of duplicate spots was obtained after global normalization between Cy3 and Cy5 signals. The gene expression level (GEL) was calculated according to the formula: GEL=FI (Cy5) of the sample/FI (Cy3) of the universal reference.

2.4. Hierarchical clustering analysis, principal component analysis, and statistical analysis

The genes whose expression was significantly different between MS and CN groups were identified by using *pierre* of the "R" statistical software system (www.cran.r-project.org) based on a Bayesian framework for analysis of microarray expression data (Baldi and Long, 2001). The error rate of this test smaller than 0.25 following the Bonferroni correction was considered as significant. Hierarchical clustering analysis and principal component analysis (PCA) were performed on a set of 286 genes differentially expressed between MS and CN groups, which were selected

Table 1
IFNβ responder/nonresponder score

Category	The parameters	Rank and score of the therapeutic response		
		Poor	Intermediate	Good
#1	Number of relapse after 2 years/number of relapse before 2 years	≧1.5	1.5–0.5	≦0.5
	Score	(−1)	0	(+1)
#2	Number of IVMP treatment after 2 years/number of IVMP treatment before 2 years	≧1.5	1.5–0.5	≦0.5
	Score	(−1)	0	(+1)
#3	Day of hospitalization after 2 years/day of hospitalization before 2 years	≧1.5	1.5–0.5	≦0.5
	Score	(−1)	0	(+1)
#4	EDSS score before treatment-EDSS score in 2 years after treatment	≦−0.5	0.5–(−0.5)	≧0.5
	Score	(−1)	0	(+1)
#5	Number of lesions on T2-weighted MRI in 2 years after treatment/number of lesions on T2-weighted MRI before treatment	≧1.2	1.2–0.8	≦0.8
	Score	(−1)	0	(+1)
#6	Patient's satisfaction	Unsatisfied	Neither satisfied nor unsatisfied	Satisfied
	Score	(−1)	0	(+1)

The total responder/nonresponder score of six categories ranges from the maximum value of +6 to the minimum value of −6. The patients with the score equal to +3 or greater than +3 were classified as responder (R), the score ranging from 0 to +2 as undetermined (UD), and the score equal to −1 or smaller than −1 as nonresponder (NR). Abbreviations: IVMP, intravenous methylprednisolone pulse.

as a discriminator for a standard × standard algorithm on GeneSpring 7.2 (Agilent Technologies, Palo Alto, CA). The differences in clinical parameters among MS subgroups were evaluated by multiple comparison test following the Bonferroni correction.

3. Results

3.1. Microarray analysis identified 286 genes differentially expressed in peripheral blood T cells between MS and control subjects

Among 1258 genes on the microarray, 286 genes were expressed differentially in peripheral blood $CD3^+$ T cells between 72 untreated MS patients and 22 CN subjects. Among them, 78 genes were upregulated, while 208 genes downregulated in MS versus CN (Supplementary Table 1 online for all datasets). We also conducted the microarray analysis of $CD3^-$ non-T cells, composed of B cells, monocytes/macrophages and NK cells, and found that 96 genes were differentially expressed in the non-T cell fraction between MS and CN (data not shown).

3.2. Hierarchical clustering analysis identified four distinct subgroups of MS and five gene classes

Hierarchical clustering analysis was performed on $CD3^+$ T-cell samples of 72 untreated MS patients and 22 CN subjects, by using the set of 286 differentially expressed genes described above as a discriminator. This unsupervised approach, which arranged the genes and samples with a similar expression pattern to make a cluster in the dendrogram, identified four distinct

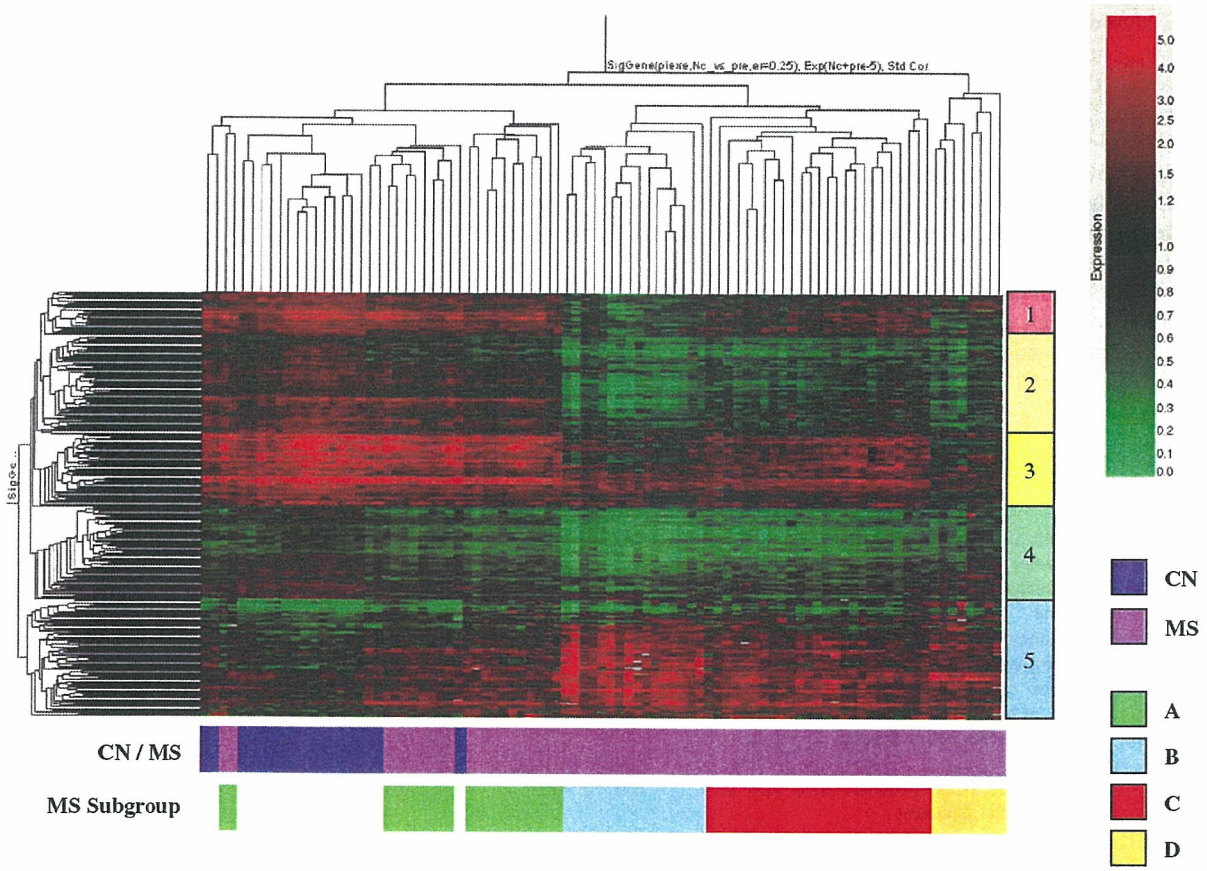

Fig. 1. Hierarchical clustering analysis of 286 genes differentially expressed between untreated MS patients and control subjects. The gene expression profile of peripheral blood $CD3^+$ T cells was studied in 72 untreated MS patients and 22 age- and sex-matched healthy control (CN) subjects, by using a 1258 cDNA microarray. Hierarchical clustering analysis was performed by selecting a set of 286 genes differentially expressed between MS and CN as a discriminator. The results are expressed in a matrix format, with each row representing the gene expression level (GEL) of a single gene in all the subjects and each column representing GEL of 286 genes in an individual subject. The matrix is shown by a pseudo-color, with red expressing upregulation, green expressing downregulation, and the color intensity representing the magnitude of the deviation from GEL 1.0 as shown on the upper right. Hierarchical clustering analysis separated MS (purple) from CN (dark blue), and classified the former into four subgroups named A (green), B (light blue), C (red) and D (yellow). The 286 genes were categorized into five classes numbered #1 (pink) to #5 (light blue).

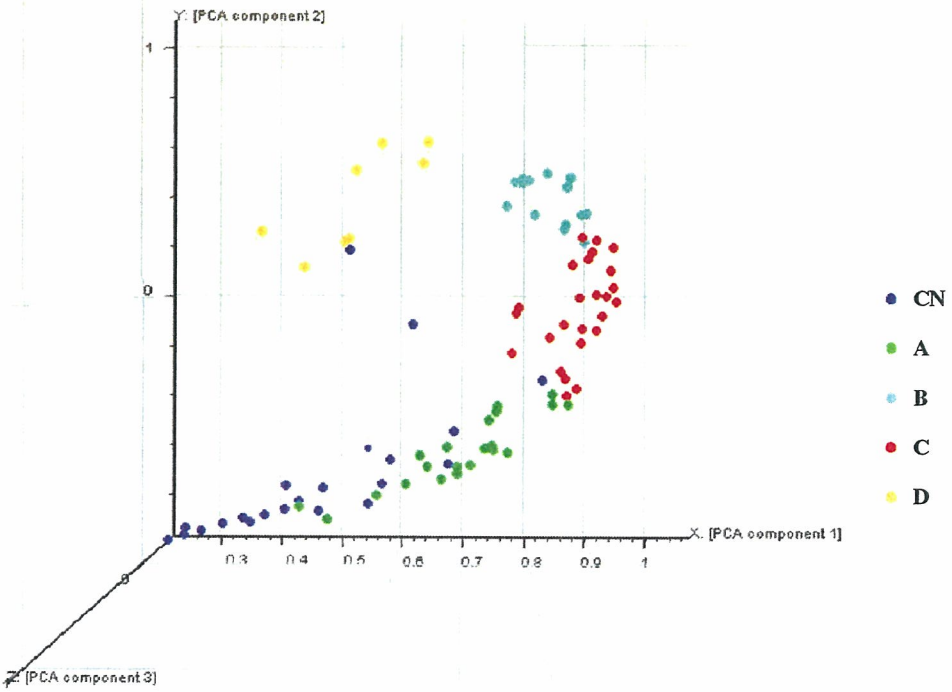

Fig. 2. Principal component analysis of 286 discriminator genes. Principal component analysis (PCA), which reduces all of the variance in the original dataset to three dimensions accounting for a significant fraction of the variance, verified a clear separation of the CN group (dark blue) and four MS subgroups named A (green), B (light blue), C (red) and D (yellow) identified by hierarchical clustering analysis.

subgroups of MS, clearly separated from the CN group (Fig. 1). We operationally designated each subgroup of MS as A, B, C and D, following the relative location in the dendrogram (Fig. 1). Principal component analysis (PCA) verified a clear discrimination of four MS subgroups and CN group (Fig. 2). Among 94 subjects examined, two MS patients and three CN subjects were considered as being unclassifiable (UC). In contrast, the clustering analysis of $CD3^-$ non-T cells did not clearly separate MS subgroups from CN (data not shown). Hierarchical clustering analysis categorized 281 of 286 differentially expressed genes into five distinct classes numbered #1 to #5 (Fig. 1 and Supplementary Table 1 online for all datasets). The remaining five, including TOP1, CHST4, SLC35A1, ST1B2, and TAF2H, were unable to be categorized into any classes. All the class #5 genes were upregulated in MS, whereas the genes of classes #1 to #4 were downregulated in MS, when compared with CN (Fig. 1). Upregulation of several class #5 genes in MS was validated by quantitative real-time RT-PCR analysis (data not shown).

3.3. Association of MS subgroups with gene clusters

Expression of the class #5 genes were elevated in all MS subgroups, whereas the classes #1 to #4 genes were downregulated in all of them, although the present study could not identify the marker genes specific for each MS subgroup. The subgroup A showed the gene expression pattern that is the most similar to CN. The similarity was supported by a partial overlap between A and CN in PCA (Fig. 2), and by the observations that one CN subject was incorporated in A, while two MS patients of A were included in CN (Fig. 1). Notably, the subgroup B showed the greatest upregulation of class #5 genes and the most prominent suppression of classes #1 to #4 genes (Fig. 1).

The class #5 genes ($n=78$) contain nine chemokines (11.5%), including CCL1, CCL3, CCL13, CCL18, CCL24, CXCL1, CXCL2, CXCL9, and CXCL14. In contrast, the classes #1 to #4 genes ($n=203$) contained only two chemokines (1.0%), such as CXCL5 and CXCL10. These observations suggest that the class #5 gene cluster is highly enriched in chemokine genes.

Fig. 3. Clinical characteristics of microarray-determined four MS subgroups. MS patients were classified into four distinct subgroups named A, B, C, and D by hierarchical clustering analysis. The bar indicates the data of individual patients. The number of relapse, the day of IVMP treatment, the day of hospitalization, and the number of lesions on T2-weighted MRI represent the data of 2 years before enrollment. Abbreviations: EDSS, Expanded Disability Status Scale; IVMP, intravenous methylprednisolone pulse; R/NR, responder/nonresponder.

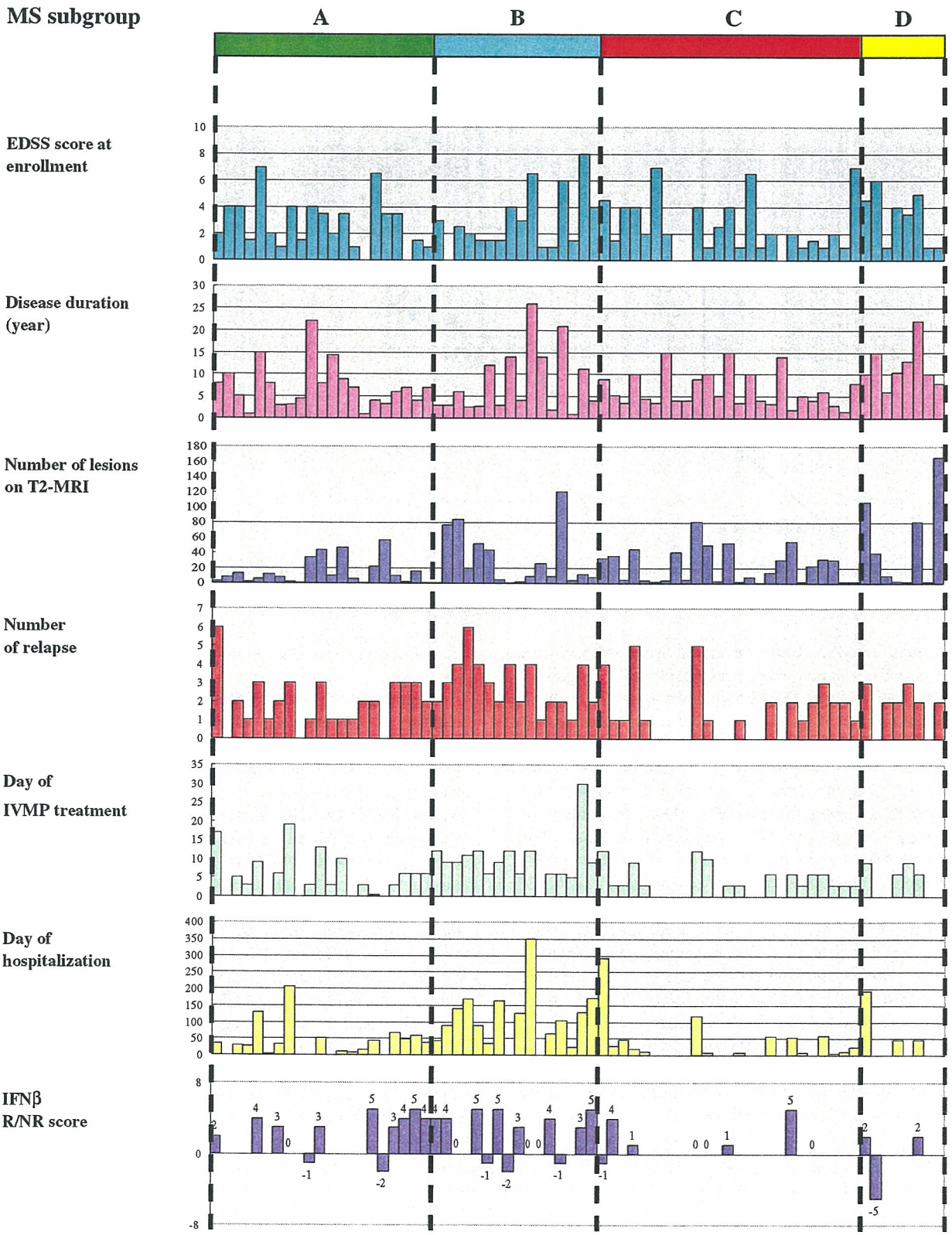
MS subgroup
A
B
C
D
EDSS score at enrollment
Disease duration (year)
Number of lesions on T2-MRI
Number of relapse
Day of IVMP treatment
Day of hospitalization
IFNβ R/NR score

Table 2
The therapeutic response to IFNβ in microarray-determined four MS subgroups

	Total	A	B	C	D	UC
IFNβ-treated patients (*n*)	46	14	14	11	5	2
Age of IFNβ-treated patients (average, SD)	34.9±9.2	33.2±7.6	36.5±10.4	33.1±8.3	36.2±13.3	41.5
Male to female ratio of IFNβ-treated patients	8 to 38	1 to 13	3 to 11	3 to 8	0 to 5	1 to 1
IFNβ responder/nonresponder score (average, SD)	1.9±2.6	2.5±2.3	2.1±2.6	1.3±2.1	−0.3±4.0	3
Dropout during a follow-up (*n*)	7	2	0	3	2	0
IFNβ responder (*n*, %)	19 (41.3%)	8 (57.1%)	8 (57.1%)	2 (18.2%)	0 (0%)	1 (50%)
IFNβ nonresponder (*n*)	7	2	3	1	1	0
Undetermined group (*n*)	13	2	3	5	2	1
The patients with IFNβ-related adverse effects (*n*, %)	29 (63.0%)	8 (57.1%)	9 (64.3%)	7 (63.6%)	4 (80%)	1 (50%)
Increase in the number of lesions on T2-weighted MRI during a follow-up (average, SD)	1.7±9.7	−2.0±7.1	2.8±6.6	7.6±15.8	−0.7±8.1	−3.5
The patients satisfied with IFNβ treatment (*n*, %)	17 (37.0%)	8 (57.1%)	6 (42.9%)	2 (18.2%)	0 (0%)	1 (50%)
The patients neither satisfied nor unsatisfied with IFNβ treatment (*n*)	21	4	7	7	2	1
The patients unsatisfied with IFNβ treatment (*n*)	8	2	1	2	3	0

Among 72 MS patients, 46 patients were treated with IFNβ for two years after enrollment. The therapeutic response was evaluated by IFNβ responder/nonresponder score shown in Table 1. Abbreviations: UC, unclassifiable.

3.4. Clinical characteristics of microarray-determined MS subgroups

Next, we investigated clinical characteristics of four MS subgroups (Supplementary Table 2 online and Fig. 3). No statistically significant differences were found among the subgroups in the age, disease duration, EDSS score, and the number of lesions on T2-weighted MRI at enrollment. However, there was a trend that the subgroup D showed a greater EDSS score and had a larger number of MRI lesions, suggestive of an advanced stage of the disease (Supplementary Table 2 online). The female outnumbered the male in all the subgroups. The male to female ratio was relatively higher in C, while no male patient was included in D. The patients with RRMS outnumbered those with SPMS in all the subgroups, although there was a mild bias for SPMS in B. The number of relapse, the day of IVMP treatment, and the day of hospitalization during preceding two years before enrollment were the largest and longest in subgroup B, and this difference was statistically significant, when compared between subgroups B and C ($p=0.0128$, 0.0183, and 0.0329 for each parameter) (Supplementary Table 2 online and Fig. 3). These observations indicate that the subgroup B included the patients who were the clinically most active before starting IFNβ.

In all MS subgroups, the conventional form of MS (CMS) greatly outnumbered non-CMS, the latter was composed of the opticospinal form (OSMS) and multifocal recurrent myelitis without optic nerve involvement. No obvious association was identified between a particular MS subgroup and the spinal cord involvement. However, 5 of 6 patients having the lesions restricted to the cerebrum (CBR) were included in subgroup C (Supplementary Table 2 online). These observations suggest that the status of T-cell gene expression might affect the lesion distribution in this subgroup.

3.5. IFN β responders were clustered in subgroups A and B

Based on the patient's own determination at enrollment, 72 MS patients were separated into two groups; 46 who started to receive IFNβ treatment for following two years, and 26 who were followed up without IFNβ treatment for successive two years (Supplementary Table 3 online). All the IFNβ-treated patients were evaluated by the IFNβ responder/nonresponder score (Table 1) at the end of the two year-treatment. They were classified into 19 IFNβ responders, 7 nonresponders, 13 undetermined subjects, and 7 dropouts (Table 2). The difference in the score among the subgroups (A: 2.5±2.3; B: 2.1±2.6; C: 1.3±2.1; and D: −0.3±4.3) did not reach the level of statistical significance (Table 2). However, there existed a trend that IFNβ responders were clustered either in subgroup A or B. Because the subgroup A contains the greatest proportion of IFNβ responders (57.1%), the patients of A were judged as being the most IFNβ responsive (Table 2). All the responders of A expressed a satisfaction on IFNβ treatment. The patients of the subgroup B also showed a good response equivalent to A (57.1%), although the number of satisfied patients was smaller. In contrast, only 2 of 11 IFNβ-treated patients in subgroup C (18.2%) and none of the patients in subgroup D were judged as IFNβ responders. The patients of C showed a trend for great increase in the number of MRI lesions during IFNβ treatment, consistent with the poor response to IFNβ (Table 2). A battery of IFNβ treatment-related adverse effects, including skin reactions, flu-like symptoms, leukocytopenia, depression, and amenorrhea, were observed in more than 50% of IFNβ-treated patients in all the subgroups (Table 2). Seven patients of the IFNβ-treated group discontinued the treatment: five due to adverse effects, one due to a severe relapse, and another by a personal reason.

We also studied T-cell gene expression profile of IFNβ-treated MS patients at 3 or 6 months after starting the

treatment. Although hierarchical clustering analysis classified these patients into several subgroups, they did not match with the subgroup A, B, C, or D determined at pretreatment (data not shown). Furthermore, no significant association was identified between these new clusters and the response to IFNβ. These observations suggest that T-cell gene expression profiling at pretreatment is the most valuable to predict the clinical outcome, whereas the analysis after starting IFNβ treatment is less informative.

3.6. Temporal profile of IFN-responsive gene expression in the first six months discriminated responders and nonresponders

Finally, we investigated the temporal expression profile of the genes with IFN-responsive promoter elements named IFN-responsive genes (IRGs) following IFNβ treatment. As we previously reported (Koike et al., 2003), IFNβ treatment for 6 months enhanced the expression of a battery of IRGs in T cells (Fig. 4). A remarkable difference was found between IFNβ responders (R) and nonresponders (NR) in the kinetics of several IRGs, such as IFN-stimulated protein 15 (ISG15), small inducible cytokine A2 (SCYA2, CCL2, or MCP-1), TNF receptor subfamily member 1B (TNFRSF1B, TNFRp75), and IFNα-inducible protein 27 (IFI27) (Fig. 5). The IFNβ responders exhibited a pattern of persistent upregulation during 6 months of the treatment. In contrast, the nonresponders showed a seesaw pattern, i.e. higher upregulation at 3 months than the responders, followed by substantial downregulation at 6 months. The differences between R and NR in the kinetics of both TNFRSF1B and IFI27 levels from 3 to 6 months were statistically significant ($p=0.0092$ and 0.0307, respectively) (Fig. 5). These observations suggest that IFNβ nonresponders also well respond to IFNβ at 3 months, but they could not maintain the responsiveness until 6 months.

4. Discussion

To elucidate the molecular basis underlying clinicopathological variability of MS, we conducted a comprehensive study that combines T-cell gene expression profiling and clinical characteristics of Japanese MS patients. Hierarchical clustering analysis of 286 genes differentially expressed between 72 untreated MS patients and 22 CN subjects classified a clinically heterogeneous population of MS into four distinct subgroups, named A, B, C, and D, and identified five gene classes numbered #1 to #5. The class

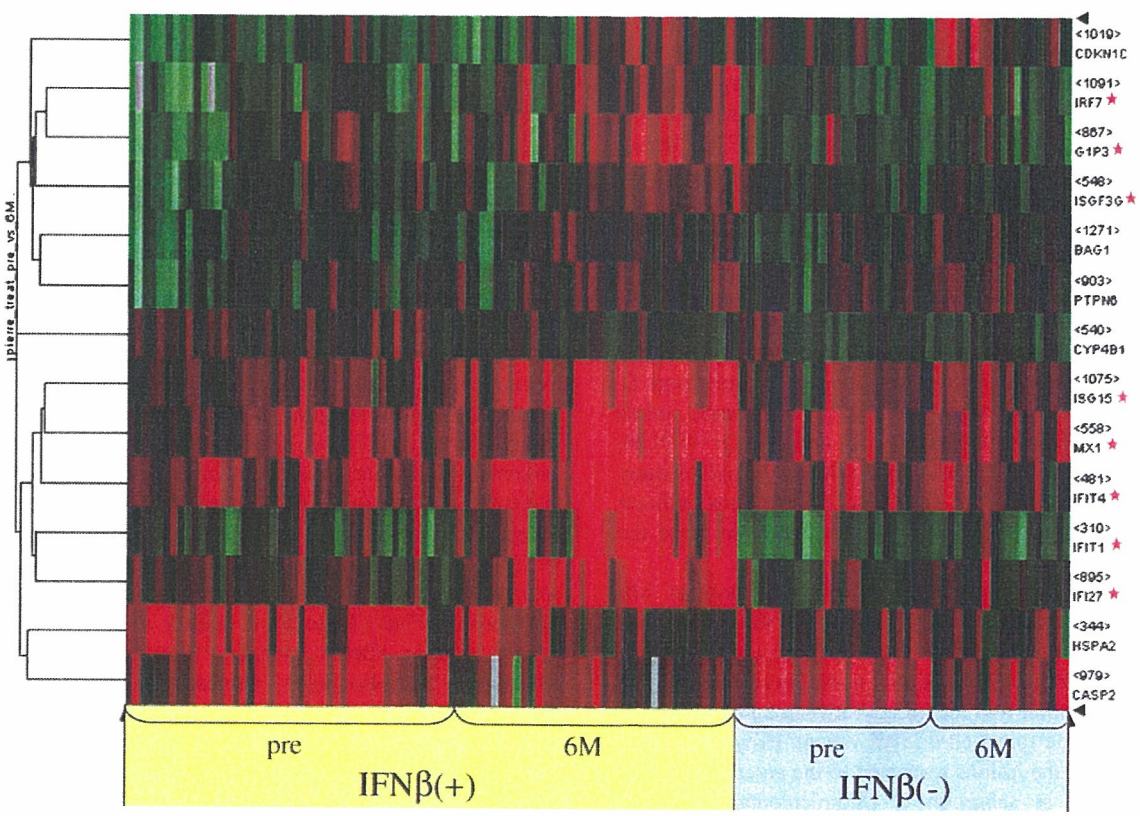

Fig. 4. Induction of IFN-responsive genes in IFNβ-treated MS patients. Seventy-two MS patients were divided into IFNβ-treated group (IFNβ+: $n=46$) and untreated group (IFNβ−; $n=26$). A cluster of known IFN-responsive genes (IRGs) indicated by the star were significantly upregulated exclusively in IFNβ-treated patients at 6 months after starting the treatment.

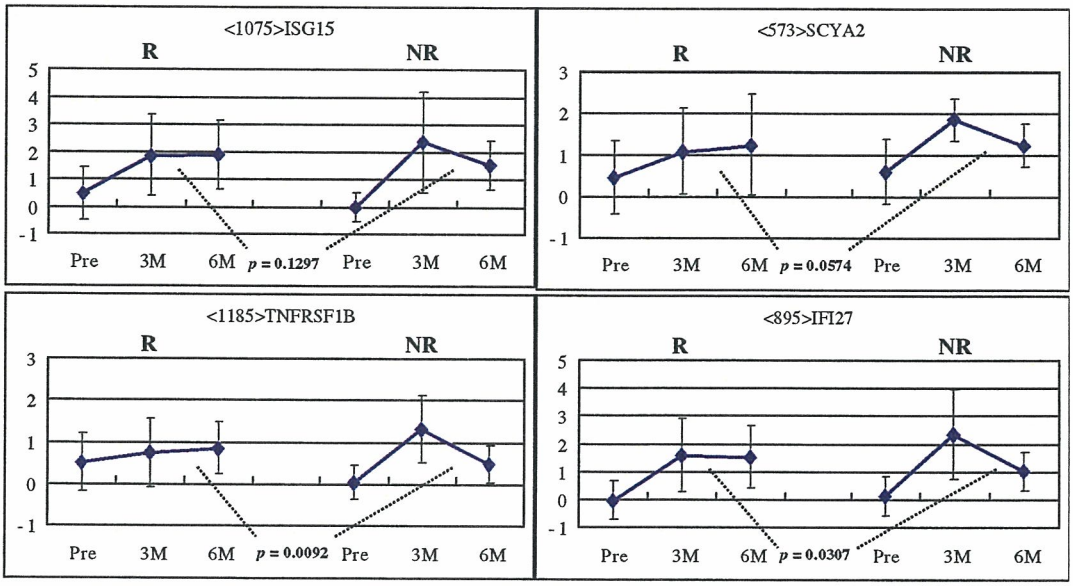

Fig. 5. Temporal profile of induction of IFN-responsive genes in IFNβ responders and nonresponders during IFNβ treatment. T-cell gene expression profiling was examined in 46 IFNβ-treated MS patients at three time points: before starting IFNβ treatment (Pre), and at 3 months (3M) and 6 months (6M) after starting the treatment. Based on the IFNβ responder/nonresponder score, they were separated into 19 IFNβ responders (R: the left) and 7 nonresponders (L: the right) as shown in Table 2. The temporal expression profile of IFN-responsive genes (IRGs), such as IFN-stimulated protein 15 (ISG15), small inducible cytokine A2 (SCYA2), TNF receptor subfamily member 1B (TNFRSF1B), and IFNα-inducible protein 27 (IFI27), is shown with the statistical differences in the kinetics during 3 to 6 months between R and NR. The vertical axis represents the gene expression level (GEL), while the horizontal axis indicates the time course.

#5 genes containing nine chemokines were upregulated exclusively in MS. The most clinically active subgroup B showed the highest upregulation of the class #5 genes. These observations suggest that the higher disease activity of B is in part attributable to overproduction of chemokines which promote lymphocyte and macrophage trafficking into the CNS (Balashow et al., 1999; Opdenakker et al., 2003). Recently, using this database as a training set for support vector machine (SVM) analysis of T cell gene expression, we found that the great majority of active RRMS patients were classified into MS subgroups, while clinically stable patients without obvious relapses for several years were occasionally classified into CN group (unpublished observations).

The class #5 genes upregulated in MS T cells include various cytokines, growth factors and their receptors, whose expression was detected at high levels in demyelinating lesions of MS, such as IL-12p40 (Windhagen et al., 1995), IL-10 (Hulshof et al., 2002), granulocyte colony-stimulating factor (GCSF) (Lock et al., 2002), platelet-derived growth factor receptor-alpha (PDGFRA) (Maeda et al., 2001), transforming growth factor-beta 2 (TGFB2) (Peress et al., 1996), and insulin-like growth factor-II (IGF-II) (Gveric et al., 1999). The class #5 genes also contain many apoptosis-signaling regulators pivotal for T cell development. It is worthy to note that nuclear receptor subfamily 4, group A, member 2 (NR4A2) in the class #5 was the most strongly upregulated gene in MS T cells. NR4A2 encodes an orphan member of the steroid–thyroid hormone receptor superfamily transcription factors designated Nurr1. Nurr1 is induced in T cells during apoptosis (Okabe et al., 1995) and the members of this family regulate clonal deletion of self-reactive T cells in the thymus (Zhou et al., 1996). Nurr1 activates the transcription of osteopontin (Lammi et al., 2004), a Th1 cytokine that plays a key role in progression of inflammatory demyelination in MS (Steinman and Zamvil, 2003). In contrast, a previous study showed that NR4A2 is downregulated in unfractionated PBMC of MS patients (Achiron et al., 2004), although the following study from the same group indicated a significant upregulation of NR4A2 in PBMC of both MS and SLE patients (Mandel et al., 2004). We validated upregulation of NR4A2 mRNA levels in MS T cells by quantitative real-time RT-PCR analysis (unpublished observations).

The present study suggests that the microarray-based classification of MS is useful to predict therapeutic response to IFNβ. The proportion of IFNβ responders greatly differed among MS subgroups: 57.1% in A, 57.1% in B, 18.2% in C and 0% in D. Furthermore, the responders are significantly different from the non-responders in the kinetics of IFN-responsive genes (IRGs). A panel of IRGs were upregulated persistently in IFNβ responders, whereas they were downregulated to some extent in nonresponders by 6 months. The precise reason for downregulation of IRGs in nonresponders after a long-term treatment remains unknown, because our study did not determine neutralizing antibody (NAb) development in individual patients. Unexpectedly, the patients of subgroup B exhibited a good response to IFNβ, despite its highest clinical activity. A recent study showed that IFNβ res-

ponders are characterized by higher relapse rates during the year prior to initiation of IFNβ treatment (Waubant et al., 2003), supporting our observations. In contrast, the patients of C with the poor response to IFNβ showed a trend for great increase in the number of MRI lesions during IFNβ treatment. A different study indicated that the number of on-treatment new T2 MRI lesions correlates with poor response to IFNβ-1a (Rudick et al., 2004), being consistent with our study. Although the subgroup D did not include any IFNβ responders, the number of MRI lesions did not increase much during the treatment, suggesting that this subgroup undergoes a neurodegenerative process independent of active inflammation (Steinman, 2001).

A number of differentially expressed genes between MS and CN include those having IFN-responsive elements in the promoter regions: p300 (EP300) and IFNα receptor 1 (IFNAR1) in the class #1, CXCL10, ATP-binding cassette (ABC) subfamily E member 1 (ABCE1 or RNS4I) (Bisbal et al., 1995), IFNγ-inducible protein 16 (IFI16), and STAT1 in the class #2, myxovirus resistance 2 (MX2) in the class #3, IFN-regulatory factors IRF9 and IRF2 in the class #4, and IFNα-16 (IFNA16) and CXCL9 (MIG) in the class #5. These observations suggest that T cells of MS patients have a constitutive defect in regulation of IFN signaling. We previously showed that CXCL9 expression was suppressed in T cells of 13 RRMS patients by a long-term treatment with IFNβ (Koike et al., 2003), suggesting that IFNβ produces a beneficial effect on MS by correcting the preexisting disturbance in the IFN-signaling pathway.

Finally, T-cell gene expression profiling identified an aberrant expression of key regulators for drug metabolism, whose role has not previously been proposed in MS (Nguyen et al., 2000). A panel of cytochrome P450 (CYP) family, which regulates Ca^{2+} influx in activated T cells (Aussel et al., 1994), were overexpressed in MS T cells. On the other hand, a wide range of ABC transporters in the classes #2, #3, and #4 were downregulated in MS T cells (see Supplementary Table 1 for all datasets). The ABC transporter superfamily regulates the transport of amino acids, ions, sugars, lipids and drugs across the cell membrane by consuming the energy derived from ATP hydrolysis. The downregulated genes in MS include ABCB1 and ABCG2 expressed on brain endothelial cells, which act as a main transporter in the blood–brain barrier and determine bioavailability of corticosteroids and mitoxantrone in the brain (Zhang et al., 2003). The clinicopathological relevance of opposing changes in CYP family enzymes and ABC transporters to MS remains to be further investigated.

In conclusion, T-cell gene expression profiling is highly valuable to identify distinct subgroups of MS associated with differential disease activity and therapeutic response to IFNβ. This approach could be applied for designing tailor-made treatment of MS.

Acknowledgements

This work was supported by grants from Research on Intractable Diseases, and Research on Psychiatric and Neurological Diseases and Mental Health, from the Ministry of Health, Labour and Welfare of Japan, Research on Health Sciences Focusing on Drug Innovation, the Japan Health Sciences Foundation (KH21101), and the Program for Promotion of Fundamental Studies in Health Sciences of the National Institute of Biomedical Innovation (NIBIO), Japan. The authors thank Drs. Masaaki Niino and Hikoaki Fukaura, Department of Neurology, Hokkaido University Graduate School of Medicine, and Dr. Masanaga Yamawaki, Department of Neurology, Tokyo Medical and Dental University for their invaluable help.

Appendix A. Supplementary data

Supplementary data associated with this article can be found, in the online version, at doi:10.1016/j.jneuroim.2006.02.004.

References

Achiron, A., Gurevich, M., Friedman, N., Kaminski, N., Mandel, M., 2004. Blood transcriptional signatures of multiple sclerosis: unique gene expression of disease activity. Ann. Neurol. 55, 410–417.

Alizadeh, A.A., Eisen, M.B., Davis, R.E., Ma, C., Lossos, I.S., Rosenwald, A., Boldrick, J.C., Sabet, H., Tran, T., Yu, X., Powell, J.I., Yang, L., Marti, G.E., Moore, T., Hudson, J. Jr., Lu, L., Lewis, D.B., Tibshirani, R., Sherlock, G., Chan, W.C., Greiner, T.C., Weisenburger, D.D., Armitage, J.O., Warnke, R., Levy, R., Wilson, W., Grever, M.R., Byrd, J.C., Botstein, D., Brown, P.O., Staudt, L.M., 2000. Distinct types of diffuse large B-cell lymphoma identified by gene expression profiling. Nature 403, 503–511.

Aussel, C., Breittmayer, J.P., Ticchioni, M., Pelassy, C., Bernard, A., 1994. Regulation of T cell activation by cytochrome P450 inhibitors. Cell. Immunol. 155, 436–445.

Balashow, K.E., Rottman, J.B., Weiner, H.L., Hancock, W.W., 1999. $CCR5^+$ and $CXCR3^+$ T cells are increased in multiple sclerosis and their ligands MIP-1α and IP-10 are expressed in demyelinating brain lesions. Proc. Natl. Acad. Sci. U. S. A. 96, 6873–6878.

Baldi, P., Long, AD., 2001. A Bayesian framework for the analysis of microarray expression data: regularized t-test and statistical inferences of gene changes. Bioinformatics 17, 509–519.

Bisbal, C., Martinand, C., Silhol, M., Lebleu, B., Salehzada, T., 1995. Cloning and characterization of a RNase L inhibitor. A new component of the interferon-regulated 2-5A pathway. J. Biol. Chem. 270, 13308–13317.

Compston, A., Coles, A., 2002. Multiple sclerosis. Lancet 359, 1221–1231.

Graumann, U., Reynolds, R., Steck, A.J., Schaeren-Wiemers, N., 2003. Molecular changes in normal appearing white matter in multiple sclerosis are characteristic of neuroprotective mechanisms against hypoxic insult. Brain Pathol. 13, 554–573.

Gveric, D., Cuzner, M.L., Newcombe, J., 1999. Insulin-like growth factors and binding proteins in multiple sclerosis plaques. Neuropathol. Appl. Neurobiol. 25, 215–225.

Hulshof, S., Montagne, L., De Groot, C.J., Van Der Valk, P., 2002. Cellular localization and expression patterns of interleukin-10,

interleukin-4, and their receptors in multiple sclerosis lesions. Glia 38, 24–35.

Jacobs, L.D., Cookfair, D.L., Rudick, R.A., Herndon, R.M., Richert, J.R., Salazar, A.M., Fischer, J.S., Goodkin, D.E., Granger, C.V., Simon, J.H., Alam, J.J., Bartoszak, D.M., Bourdette, D.N., Braiman, J., Brownscheidle, C.M., Coats, M.E., Cohan, S.L., Dougherty, D.S., Kinkel, R.P., Mass, M.K., Munschauer, F.E. III, Priore, R.L., Pullicino, P.M., Scherokman, B.J., Weinstock-Guttman, B., Whitham, R.H., 1996. Intramuscular interferon beta-1a for disease progression in relapsing multiple sclerosis. The Multiple Sclerosis Collaborative Research Group (MSCRG). Ann. Neurol. 39, 285–294.

Jacobs, L.D., Beck, R.W., Simon, J.H., Kinkel, R.P., Brownscheidle, C.M., Murray, T.J., Simonian, N.A., Slasor, P.J., Sandrock, A.W., 2000. Intramuscular interferon beta-1a therapy initiated during a first demyelinating event in multiple sclerosis. CHAMPS study group. N. Engl. J. Med. 343, 898–904.

Koike, F., Satoh, J., Miyake, S., Yamamoto, T., Kawai, M., Kikuchi, S., Nomura, K., Yokoyama, K., Ota, K., Kanda, T., Fukazawa, T., Yamamura, T., 2003. Microarray analysis identifies interferon β-regulated genes in multiple sclerosis. J. Neuroimmunol. 139, 109–118.

Lammi, J., Huppunen, J., Aarnisalo, P., 2004. Regulation of the osteopontin gene by the orphan nuclear receptor NURR1 in osteoblasts. Mol. Endocrinol. 18, 1546–1557.

Lock, C., Hermans, G., Pedotti, R., Brendolan, A., Schadt, E., Garren, H., Langer-Gould, A., Strober, S., Cannella, B., Allard, J., Klonowski, P., Austin, A., Lad, N., Kaminski, N., Galli, S.J., Oksenberg, J.R., Raine, C.S., Heller, R., Steinman, L., 2002. Gene-microarray analysis of multiple sclerosis lesions yields new targets validated in autoimmune encephalomyelitis. Nat. Med. 8, 500–508.

Lucchinetti, C., Brück, W., Parisi, J., Scheithauer, B., Rodriguez, M., Lassmann, H., 2000. Heterogeneity of multiple sclerosis lesions: implications for the pathogenesis of demyelination. Ann. Neurol. 47, 707–717.

Maeda, Y., Solanky, M., Menonna, J., Chapin, J., Li, W., Dowling, P., 2001. Platelet-derived growth factor-α receptor-positive oligodendroglia are frequent in multiple sclerosis lesions. Ann. Neurol. 49, 776–785.

Mandel, M., Gurevich, M., Pauzner, R., Kaminski, N., Achiron, A., 2004. Autoimmunity gene expression portrait: specific signature that intersects or differentiates between multiple sclerosis and systemic lupus erythematosus. Clin. Exp. Immunol. 138, 164–170.

McDonald, W.I., Compston, A., Edan, G., Goodkin, D., Hartung, H.P., Lublin, F.D., McFarland, H.F., Paty, D.W., Polman, C.H., Reingold, S.C., Sandberg-Wollheim, M., Sibley, W., Thompson, A., van den Noort, S., Weinshenker, B.Y., Wolinsky, J.S., 2001. Recommended diagnostic criteria for multiple sclerosis: guidelines from the international panel on the diagnosis of multiple sclerosis. Ann. Neurol. 50, 121–127.

Nguyen, L.T., Ramanathan, M., Weinstock-Guttman, B., Dole, K., Miller, C., Planter, M., Patrick, K., Brownscheidle, C., Jacobs, L.D., 2000. Detection of cytochrome P450 and other drug-metabolizing enzyme mRNAs in peripheral blood mononuclear cells using DNA arrays. Drug Metab. Dispos. 28, 987–993.

Okabe, T., Takayanagi, R., Imasaki, K., Haji, M., Nawata, H., Watanabe, T., 1995. cDNA cloning of a NGFI-B/nur77-related transcription factor from an apoptotic human T cell line. J. Immunol. 154, 3871–3879.

Opdenakker, G., Nelissen, I., Van Damme, J., 2003. Functional roles and therapeutic targeting of gelatinase B and chemokines in multiple sclerosis. Lancet Neurol. 2, 747–756.

Panitch, H.S., Hirsch, R.L., Schindler, J., Johnson, K.P., 1987. Treatment of multiple sclerosis with gamma interferon: exacerbations associated with activation of the immune function. Neurology 37, 1097–1102.

Peress, N.S., Perillo, E., Seidman, R.J., 1996. Glial transforming growth factor (TGF)-β isotypes in multiple sclerosis: differential glial expression of TGF-β1, 2 and 3 isotypes in multiple sclerosis. J. Neuroimmunol. 71, 115–123.

Rudick, R.A., Lee, J.-C., Simon, J., Ransohoff, R.M., Fisher, E., 2004. Defining interferon β response status in multiple sclerosis patients. Ann. Neurol. 56, 548–555.

Saida, T., Tashiro, K., Itoyama, Y., Sato, T., Ohashi, Y., Zhao, Z., the Interferon Beta-1b Multiple Sclerosis Study Group of Japan, 2005. Interferon beta-1b is effective in Japanese RRMS patients. A randomized, multicenter study. Neurology 64, 621–630.

Satoh, J., Nakanishi, M., Koike, F., Miyake, S., Yamamoto, T., Kawai, M., Kikuchi, S., Nomura, K., Yokoyama, K., Ota, K., Kanda, T., Fukazawa, T., Yamamura, T., 2005. Microarray analysis identifies an aberrant expression of apoptosis and DNA damage-regulatory genes in multiple sclerosis. Neurobiol. Dis. 18, 537–550.

Staudt, L.M., 2001. Gene expression physiology and pathophysiology of the immune system. Trends Immunol. 22, 35–40.

Steinman, L., 2001. Multiple sclerosis: a two-stage disease. Nature Immunol. 2, 762–764.

Steinman, L., Zamvil, S., 2003. Transcriptional analysis of targets in multiple sclerosis. Nat. Rev., Immunol. 3, 483–492.

Stürzbecher, S., Wandinger, K.P., Rosenwald, A., Sathyamoorthy, M., Tzou, A., Mattar, P., Frank, J.A., Staudt, L., Martin, R., McFarland, H.F., 2003. Expression profiling identifies responder and non-responder phenotypes to interferon-β in multiple sclerosis. Brain 126, 1219–1429.

Tajouri, L., Mellick, A.S., Ashton, K.J., Tannenberg, A.E., Nagra, R.M., Tourtellotte, W.W., Griffiths, L.R., 2003. Quantitative and qualitative changes in gene expression patterns characterize the activity of plaques in multiple sclerosis. Mol. Brain Res. 119, 170–183.

The IFNB Multiple Sclerosis Study Group, 1993. Interferon beta-1b is effective in relapsing–remitting multiple sclerosis. I. Clinical results of a multicenter, randomized, double-blind, placebo-controlled trial. Neurology 43, 655–661.

van de Vijver, M.J., He, Y.D., van't Veer, L.J., Dai, H., Hart, A.A., Voskuil, D.W., Schreiber, G.J., Peterse, J.L., Roberts, C., Marton, M.J., Parrish, M., Atsma, D., Witteveen, A., Glas, A., Delahaye, L., van der Velde, T., Bartelink, H., Rodenhuis, S., Rutgers, E.T., Friend, S.H., Bernards, R., 2000. A gene-expression signature as a predictor of survival in breast cancer. N. Engl. J. Med. 347, 1999–2009.

Waubant, E., Vukusic, S., Gignoux, L., Dubief, F.D., Achiti, I., Blanc, S., Renoux, C., Confavreux, C., 2003. Clinical characteristics of responders to interferon therapy for relapsing MS. Neurology 61, 184–189.

Windhagen, A., Newcombe, J., Dangond, F., Strand, C., Woodroofe, M.N., Cuzner, M.L., Hafler, D.A., 1995. Expression of costimulatory molecules B7-1 (CD80), B7-2 (CD86), and interleukin 12 cytokine in multiple sclerosis lesions. J. Exp. Med. 182, 1985–1996.

Zhou, T., Cheng, J., Yang, P., Wang, Z., Liu, C., Su, X., Bluethmann, H., Mountz, J., 1996. Inhibition of Nur77/Nurr1 leads to inefficient clonal deletion of self-reactive T cells. J. Exp. Med. 183, 1879–1892.

Zhang, W., Mojsilovic-Petrovic, J., Andrade, M.F., Zhang, H., Ball, M., Stanimirovic, D.B., 2003. The expression and functional characterization of ABCG2 in brain endothelial cells and vessels. FASEB J. 17, 2085–2087.

BMC Neurology

BioMed Central

Research article

Open Access

Microarray analysis identifies a set of CXCR3 and CCR2 ligand chemokines as early IFNβ-responsive genes in peripheral blood lymphocytes *in vitro*: an implication for IFNβ-related adverse effects in multiple sclerosis

Jun-ichi Satoh*[1,2], Yusuke Nanri[2], Hiroko Tabunoki[1] and Takashi Yamamura[2]

Address: [1]Department of Bioinformatics, Meiji Pharmaceutical University, 2-522-1 Noshio, Kiyose, Tokyo 204-8588, Japan and [2]Department of Immunology, National Institute of Neuroscience, NCNP, 4-1-1 Ogawahigashi, Kodaira, Tokyo 187-8502, Japan

Email: Jun-ichi Satoh* - satoj@ncnp.go.jp; Yusuke Nanri - nanriyu@cc.saga-u.ac.jp; Hiroko Tabunoki - tabunoki@my-pharm.ac.jp; Takashi Yamamura - yamamura@ncnp.go.jp

* Corresponding author

Published: 19 May 2006

BMC Neurology 2006, **6**:18 doi:10.1186/1471-2377-6-18

Received: 20 March 2006
Accepted: 19 May 2006

This article is available from: http://www.biomedcentral.com/1471-2377/6/18

Abstract

Background: A substantial proportion of multiple sclerosis (MS) patients discontinue interferon-beta (IFNβ) treatment due to various adverse effects, most of which emerge at the early phase after initiation of the treatment and then diminish with time. At present, the molecular mechanism underlying IFNβ-related adverse effects remains largely unknown. The aim of this study is to identify a comprehensive list of early IFNβ-responsive genes (IRGs) in peripheral blood mononuclear cells (PBMC) that may play a key role in induction of adverse effects.

Methods: Total RNA of PBMC exposed to 50 ng/ml recombinant human IFNβ for 3 to 24 hours *in vitro* was processed for cDNA microarray analysis, followed by quantitative real-time RT-PCR analysis.

Results: Among 1,258 genes on the array, IFNβ elevated the expression of 107 and 87 genes, while it reduced the expression of 22 and 23 genes at 3 and 24 hours, respectively. Upregulated IRGs were categorized into conventional IFN-response markers, components of IFN-signaling pathways, chemokines, cytokines, growth factors, and their receptors, regulators of apoptosis, DNA damage, and cell cycle, heat shock proteins, and costimulatory and adhesion molecules. IFNβ markedly upregulated CXCR3 ligand chemokines (SCYB11, SCYB10 and SCYB9) chiefly active on effector T helper type 1 (Th1) T cells, and CCR2 ligand chemokines (SCYA8 and SCYA2) effective on monocytes, whereas it downregulated CXCR2 ligand chemokines (SCYB2, SCYB1 and IL8) primarily active on neutrophils.

Conclusion: IFNβ immediately induces a burst of gene expression of proinflammatory chemokines *in vitro* that have potential relevance to IFNβ-related early adverse effects in MS patients *in vivo*.